Numerical methods: time-domain approaches

Didier Dragna

Laboratoire de Mécanique des Fluides et d'Acoustique
UMR CNRS 5509 - École Centrale de Lyon
didier.dragna@ec-lyon.fr

14 June 2018,
CeLyA Summer School 2018 on Atmospheric Sound Propagation
Valpré, Écully

http://acoustique.ec-lyon.fr

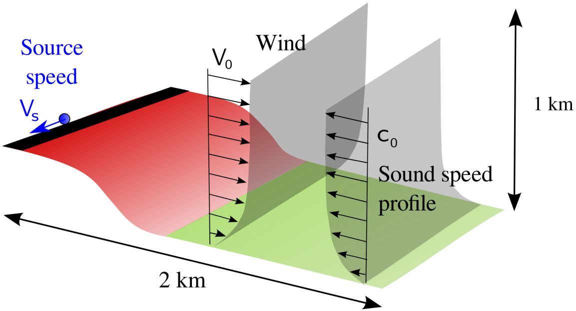

Outdoor sound propagation

interaction with the ground:

- reflexion over an absorbing ground
- diffraction due to the terrain profile and/or obstacles (screens, ...)

inhomogeneous atmosphere:

- wind profile
- temperature
- diffusion by atmospheric turbulence

Transportation noise

- broadband noise
- moving source
- propagation range up to 5 km

Context: Interest of time-domain approaches

Time-domain approaches for outdoor sound propagation:

- development for twenty years [1-3]
- due to the growth of computational power

Broadband computation

- single run $\Longrightarrow$ results over a frequency band

Sources in motion are simply taken into account

- Doppler effect + convective amplification

Outputs are time-domain signals

- one can hear the results
- interest for perception and auralization

Adapted for pulse signals (ex: transient signals, blast waves, ...)

Nonlinear effects

Time-domain equations (1)

Several set of equations possible for studying sound propagation in the atmosphere:

- the full Navier-Stokes equations

  ex: predicting infrasound propagating in the upper atmosphere where nonlinear and thermoviscous effects can be important

Study by Sabatini *et al.* [4]

Infrasonic source located on the ground

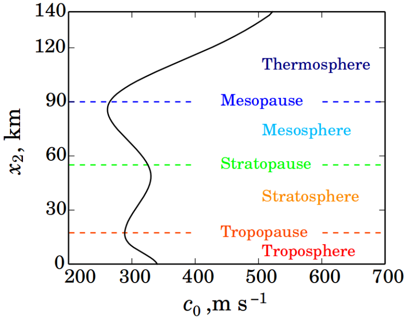

Sound speed profile in the atmosphere

Time-domain equations (1)

Several set of equations possible for studying sound propagation in the atmosphere:

- the full Navier-Stokes equations

  ex: predicting infrasound propagating in the upper atmosphere where nonlinear and thermoviscous effects can be important

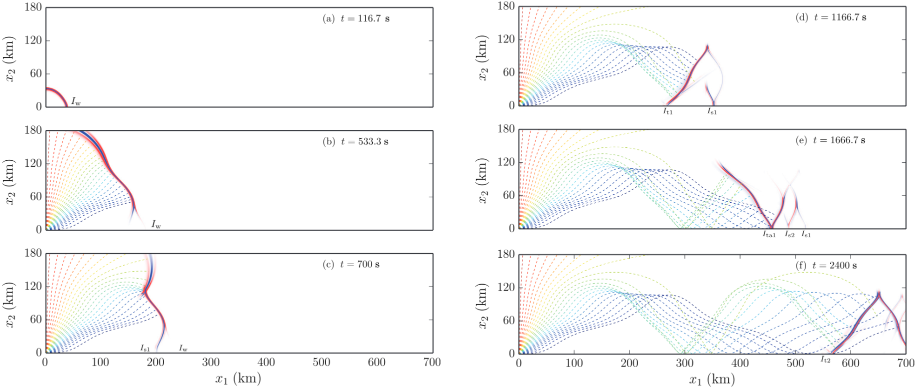

Snapshots of the normalized pressure + acoustic rays superimposed

- the full Euler equations
  ex: predicting blast wave propagation, **sonic boom**

Study by Yamashita & Suzuki [5]

Flight altitude: 6 km - Mach number: 1.4

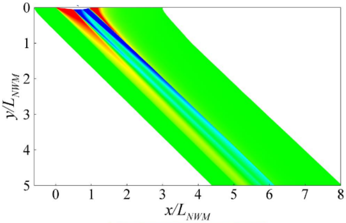

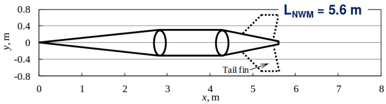

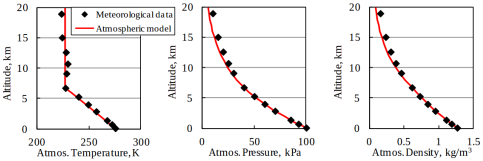

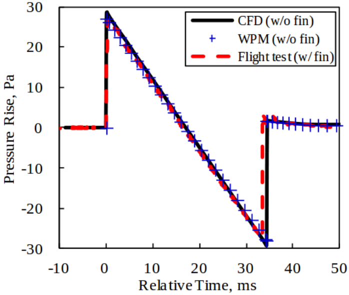

Time-domain equations (3)

In most common cases in atmospheric sound propagation,
propagation is a linear process and thermoviscous effects can be neglected
$\Longrightarrow$ one can linearize the Euler equations around the ambient values

Linearized Euler equations (LEEs) for atmospheric sound propagation: [3]

$$\frac{\partial p}{\partial t} + \mathbf{V}_0.\nabla p + \rho_0 c_0^2 \nabla.\mathbf{v} = \rho_0 c_0^2 Q,$$
$$\rho_0 \frac{\partial \mathbf{v}}{\partial t} + \rho_0 (\mathbf{V}_0.\nabla)\mathbf{v} + \rho_0 (\mathbf{v}.\nabla)\mathbf{V}_0 + \nabla p = \mathbf{R}.$$

Acoustic variables

p acoustic pressure

$\mathbf{v}$ acoustic velocity

Medium properties

ρ_0 density

$\mathbf{V}_0$ mean flow = wind

c_0 sound speed

Source terms

Q mass source
$\approx$ monopolar source

$\mathbf{R}$ external forces
$\approx$ dipolar source

Other possible forms: 3 equations on (p, ρ, $\mathbf{v}$), ...

Equations written in conservative form:

$$\frac{\partial \mathbf{U}}{\partial t} + \frac{\partial \mathbf{E}}{\partial x} + \frac{\partial \mathbf{F}}{\partial y} + \frac{\partial \mathbf{G}}{\partial z} + \mathbf{H} = \mathbf{S},$$

Comparison with other numerical approaches

	Temperature profile	Wind profile	Reflexion over the ground	Diffraction (topography, obstacles, ...)
Geometrical methods				
Ray-tracing + Geometrical theory of diffraction	+++	+++	+++	+++
Wave-based methods				
Paraxial approximations	+++	+++	+++	+
Boundary element method (BEM)	+	+	+++	+++
Transmission Line Matrix (TLM) [6]	+++	+	+++	+++
Linearized Euler equations (LEEs)	+++	+++	+++	+++
...				

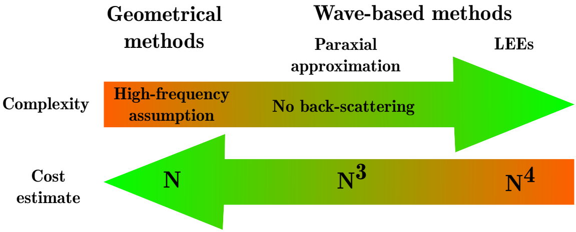

Discretization in time and space

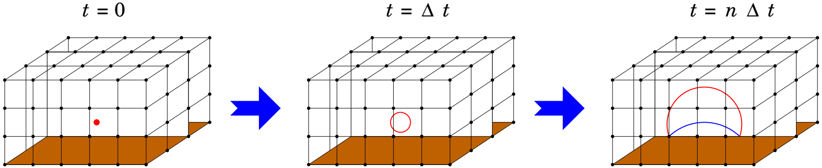

Basic idea to solve $\dfrac{\partial \mathbf{U}}{\partial t} = K(\mathbf{U})$ with $K(\mathbf{U}) = \mathbf{S} - \dfrac{\partial \mathbf{E}}{\partial x} - \dfrac{\partial \mathbf{F}}{\partial y} - \dfrac{\partial \mathbf{G}}{\partial z} - \mathbf{H}$

1. we set the initial conditions $\mathbf{U}(t = 0)$
2. we compute the spatial derivatives of the fluxes $\dfrac{\partial \mathbf{E}}{\partial x}$, $\dfrac{\partial \mathbf{F}}{\partial y}$ and $\dfrac{\partial \mathbf{G}}{\partial z}$ to evaluate $K(\mathbf{U})$
3. we integrate in time to obtain $\mathbf{U}(t = \Delta t)$

....

n. we obtain $\mathbf{U}(t = n\Delta t)$

Numerical methods for the LEEs (2)

To solve the LEEs, we need:

- a numerical differential method
- a time-integration method

Numerous numerical methods available in the literature:

- numerical differentiation methods
  - **finite differences**
  - pseudospectral methods [7]
  - finite element method
  - finite volume method
  - ....

- time-integration methods
  - **Runge-Kutta algorithms**
  - Adams-Bashforth algorithm
  - ....

Hereafter, the presentation is restricted to finite-difference methods and Runge-Kutta algorithms

Remark:
- the acronym FDTD (for finite-difference time-domain) is usually employed when time-domain equations are solved using finite difference methods to evaluate the spatial derivatives

Finite difference methods: standard schemes (1)

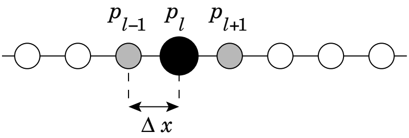

Taylor series expansion:

$$p_{l-1} = p_l - \Delta x \left.\frac{\partial p}{\partial x}\right|_l + \frac{\Delta x^2}{2} \left.\frac{\partial^2 p}{\partial x^2}\right|_l - \frac{\Delta x^3}{6} \left.\frac{\partial^3 p}{\partial x^3}\right|_l + \dots$$

$$p_{l+1} = p_l + \Delta x \left.\frac{\partial p}{\partial x}\right|_l + \frac{\Delta x^2}{2} \left.\frac{\partial^2 p}{\partial x^2}\right|_l + \frac{\Delta x^3}{6} \left.\frac{\partial^3 p}{\partial x^3}\right|_l + \dots$$

$\Longrightarrow$ standard scheme with a 3-points second-order stencil

$$\left.\frac{\partial p}{\partial x}\right|_l = \frac{p_{l+1} - p_{l-1}}{2\Delta x} + O(\Delta x^2)$$

Higher order schemes are obtained by keeping more terms in the Taylor series

Finite difference methods: standard schemes (2)

Ex: 5-points fourth-order standard scheme

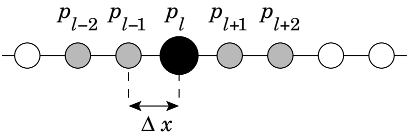

$$\left.\frac{\partial p}{\partial x}\right|_l = \frac{1}{\Delta x}\left[-\frac{1}{12}(p_{l+2} - p_{l-2}) + \frac{2}{3}(p_{l+1} - p_{l-1})\right] + O(\Delta x^4)$$

General formula for schemes over a $2N + 1$ points stencil:

$$\left.\frac{\partial p}{\partial x}\right|_l = \frac{1}{\Delta x}\sum_{j=1}^{N} a_j(p_{l+j} - p_{l-j})$$

For a harmonic wave $p = \exp(\mathrm{i}kx)$:

- its derivative: $\left.\dfrac{\partial p}{\partial x}\right|_l = \mathrm{i}kp$

- its finite difference approximation:

$$\underbrace{\left.\frac{\partial p}{\partial x}\right|_l}_{\mathrm{i}k^* p} = \frac{2\mathrm{i}}{\Delta x}\sum_{j=1}^{N} a_j \sin(jk\Delta x)p$$

Notion of effective wave number:

$$k^*\Delta x = 2\sum_{j=1}^{N} a_j \sin(jk\Delta x)$$

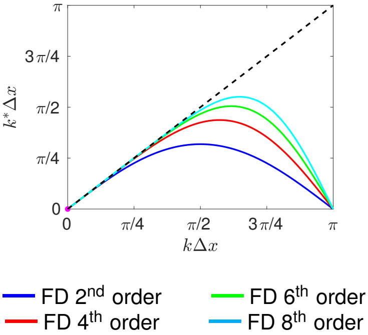

Long wavelengths ($k\Delta x < \pi/8$ corresponding to a resolution $\lambda/\Delta x$ of at least 16 points per wavelength) are sufficiently discretized and $k^* \approx k$

For short wavelengths ($\pi/8 < k\Delta x < \pi$), $k^* \neq k$; increasing the order of FD schemes allows one to reduce the error

Note that the maximal wavenumber is $k = \Delta x/\pi$ corresponding to two points per walength

Finite difference methods: effective wave number (2)

Dispersion relation for the advection equation: $\dfrac{\partial p}{\partial t} + c_0 \dfrac{\partial p}{\partial x} = 0$

- exact equation: $\omega = c_0 k$

- finite difference approximation: $\omega = c_0 k^*(k\Delta x)$

Dispersion relation modified by the finite difference approximation

Ex: propagation of a harmonic wave

$\dfrac{\partial p}{\partial t} + c_0 \dfrac{\partial p}{\partial x} = 0$ with $p(t=0) = \exp(\mathrm{i}kx)$

Analytical solution: $p_{\mathrm{ana}}(x,t) = \exp(\mathrm{i}kx - \mathrm{i}kc_0 t)$

Numerical solution: $p_{\mathrm{num}}(x,t) = \exp(\mathrm{i}kx - \mathrm{i}k^* c_0 t)$
$= p_{\mathrm{ana}}(x,t)\exp[-\mathrm{i}(k^* - k)c_0 t]$

At $x = n\Delta x$, the signal recorded at the time $t = x/c_0$ is:

$p_{\mathrm{num}}(x, t = x/c_0) = p_{\mathrm{ana}}(x, t = x/c_0)\exp[-\mathrm{i}n(k^* - k)\Delta x]$

$\Longrightarrow$ phase error that increases as the propagation time increases

Finite difference methods: optimized schemes

Schemes used in computational aeroacoustics

High order + Large stencil with coefficients a_j optimized to miminize the numerical error over a given range of wavenumber:

- optimization for $0 \leq k\Delta x \leq \pi/2$ in Tam & Webb [8]
- optimization for $\pi/16 \leq k\Delta x \leq \pi/2$ in Bogey & Bailly [9]

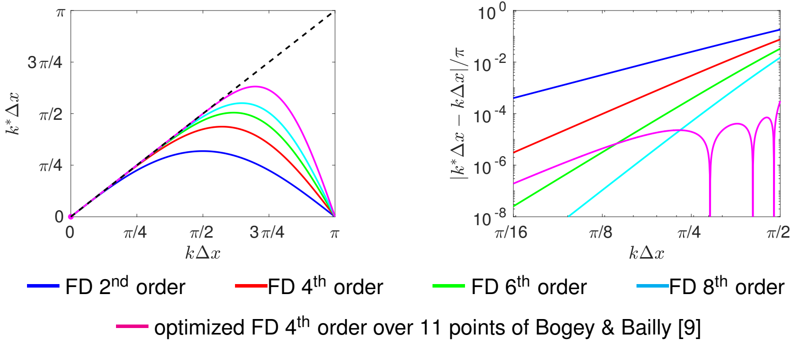

Error on the phase lower than 10 %
($|k\Delta x - k^*\Delta x| \leq 0.10\pi$)

Number of points per wavelength:

- is very large for low order schemes
- decreases as the order increases

Example: $f = 340$ Hz, $\lambda = 1$ m
propagation distance 100 m

- 2nd order: $\lambda/\Delta x \approx 115 \Longrightarrow$ 11500 points
- 4th order: $\lambda/\Delta x \approx 18 \Longrightarrow$ 1800 points
- 8th order: $\lambda/\Delta x \approx 7 \Longrightarrow$ 700 points
- optimized 4th order: $\lambda/\Delta x \approx 4 \Longrightarrow$ 400 points

Long-range propagation:

- propagation over a large number of wavelengths
- high-order schemes mandatory, especially for 3D computations

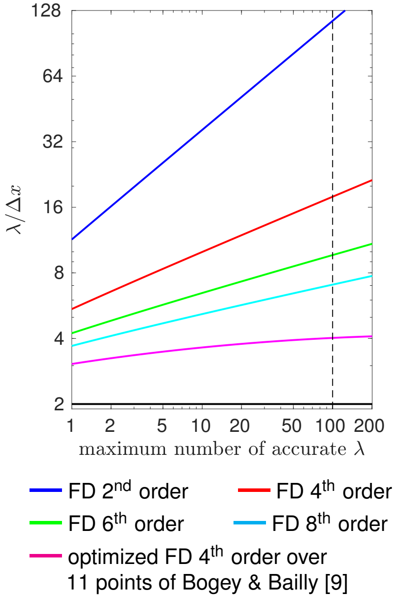

Time-integration method: Runge-Kutta algorithm

First-order differential equation of the form $\dfrac{\partial u}{\partial t} = F(u)$ can be integrated in time using explicit Runge-Kutta algorithms (among others)

- value of u at the n th time step Δt : $u(n\Delta t) = u_n$
- u_0 is given and succesive iterations are performed to obtain u_n

Low storage p-stages Runge-Kutta algorithm:

$$
\begin{aligned}
u^{(0)} &= u_n, \\
u^{(l)} &= u_n + \alpha_l \, \Delta t \, F\left(u^{(l-1)}\right), \text{ for } 1 \leq l \leq p \\
u_{n+1} &= u^{(p)}.
\end{aligned}
$$

Standard schemes of order p

- coefficients α_l obtained from Taylor series
- order 4 usually chosen

Optimized schemes

- high order
- coefficients α_l optimized in the frequency space: accuracy + stability

Harmonic wave: $u = \exp(\mathrm{i}kx - \mathrm{i}\omega t)$

Amplification factor:

- exact: $\dfrac{u_{n+1}}{u_n} = \exp(-\mathrm{i}\omega\Delta t)$
- with RK method: $\dfrac{u_{n+1}}{u_n} = |G(\omega\Delta t)| \exp(-\mathrm{i}\omega^*\Delta t)$

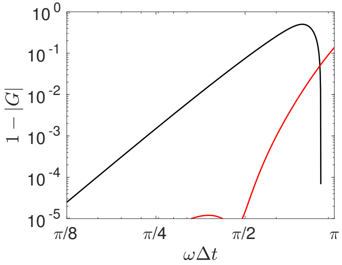

Dissipation error

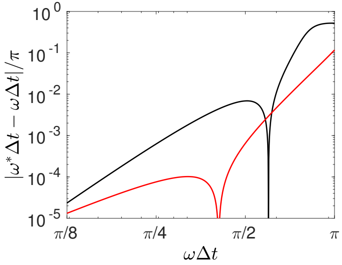

Phase error

standard 4-stage 4^{th} order RK

optimized 6-stage 2^{nd} order RK of Bogey & Bailly [9]

Time-integration method: Stability

Harmonic wave: $u = \exp(\mathrm{i}kx - \mathrm{i}\omega t)$

Amplification factor:
$$\frac{u_{n+1}}{u_n} = |G(\omega\Delta t)| \exp(-\mathrm{i}\omega^* \Delta t)$$

Instability if $|G(\omega\Delta t)| > 1$

or $\omega\Delta t > (\omega\Delta t)_{\max}$

ex: standard 4$^{\text{th}}$ order RK, $\omega\Delta t < 2.8$

Dispersion relation:
$\omega = kc_0$ or $\omega\Delta t = k\Delta x$ CFL with

the Courant-Friedrichs-Lewy number:
$$\text{CFL} = \frac{c_0\Delta t}{\Delta x}$$

Maximal possible value of $k\Delta x$ is π

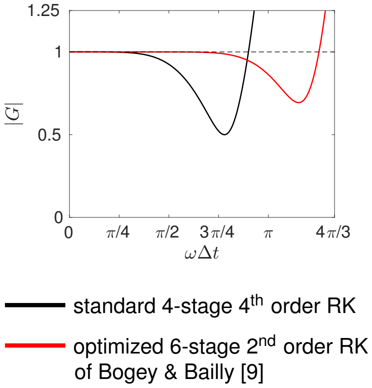

$\Longrightarrow$ instability occurs if $\text{CFL} > \text{CFL}_{\max}$ with $\text{CFL}_{\max} = (\omega\Delta t)_{\max}/\pi$

ex: standard 4$^{\text{th}}$ order RK, $\text{CFL}_{\max} \approx 0.9$

Actually, because the dispersion relation is $\omega = k^* c_0$, $\text{CFL}_{\max}$ depends on both the time-integration method and the differentiation method

Non-reflecting boundary conditions

Computational domain in volume-discretization methods needs to be truncated

$\Longrightarrow$ at the open boundaries, need to have a reflection-free boundary condition

Two widely spread methods:

- perfectly matched layers
- non-reflecting boundary condition of Tam and Dong

Numerous other possible methods!

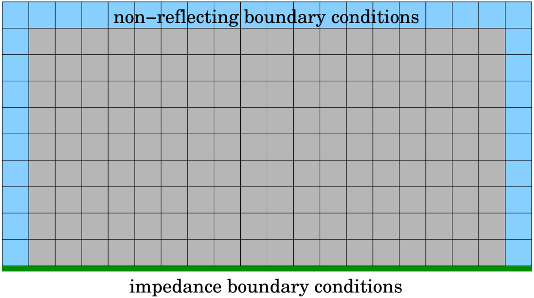

Principle: use an absorbing layer at the outer boundaries which do not generate reflected waves at the interface [10]

Change of variable:

$$x \to x + \frac{\mathrm{i}}{\omega}\int_{x_0}^{x} \sigma \mathrm{d}x$$

$\sigma > 0$ in the PML and null elsewhere

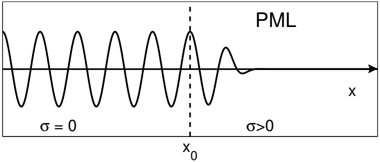

Harmonic wave:

$$p = \exp(\mathrm{i}kx - \mathrm{i}\omega t) \qquad \Longrightarrow \qquad p = \exp\left(\mathrm{i}kx - \mathrm{i}\omega t - \frac{k}{\omega}\int_{x_0}^{x} \sigma \mathrm{d}x\right)$$

Ex : 1-D advection equation

$$\frac{\partial p}{\partial t} + c_0 \frac{\partial p}{\partial x} = 0 \qquad \Longrightarrow \qquad \frac{\partial p}{\partial t} + c_0 \frac{\partial p}{\partial x} + \sigma p = 0$$

Method:

- very efficient
- unstable in the presence of a mean flow

Principle: in the farfield, propagative waves of the form: [11,12]

$p \approx F(r/v_g - t)$

$\mathbf{v} \approx F(r/v_g - t)\mathbf{e_r}$

with v_g the group velocity

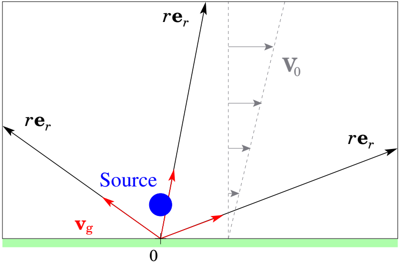

Solution of the equations:

$$\frac{\partial p}{\partial t} + v_g \left(\frac{\partial}{\partial r} + \frac{1}{r} \right) p = 0,$$
$$\frac{\partial \mathbf{v}}{\partial t} + v_g \left(\frac{\partial}{\partial r} + \frac{1}{r} \right) \mathbf{v} = 0.$$

The above equations are solved instead of the LEEs at the outer boundaries

Method:

- very efficient, even on the presence of a mean flow
- requires however to specify the location of the source region
  difficult to apply if there are multiple sources or moving sources

Numerical techniques for long-range computations (1)

Volume discretization methods are very costly for lange-range computations

Some numerical techniques can be employed to reduce their cost:

1. For impulsive sources, the acoustic signal usually has only a limited spatial extent

$\Longrightarrow$ **moving window**: reduce the computational domain to a small domain around the pulse that moves with it [2,7]

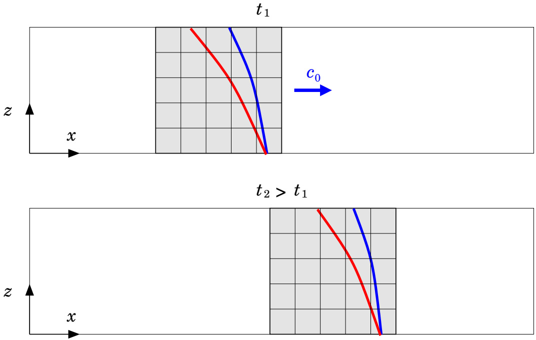

Numerical techniques for long-range computations (2)

2. **Coupling between the LEEs and the parabolic equation**

- near-field: resolution of the LEEs which allow to account precisely of diffraction by obstacles (including back-scattering) and of complex wind fields
- far-field: resolution of the parabolic equation, which is more efficient for long-range computations

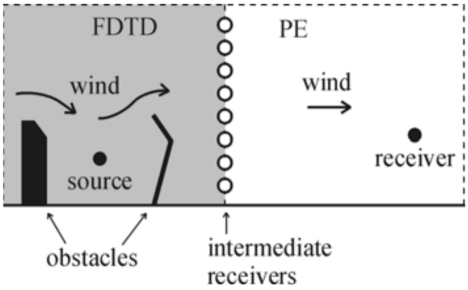

Example of application in Van Renterghem et al. [13]

Two possible approaches:

- locally-reacting ground
  $\Longrightarrow$ reflection over the ground can be modelled through a surface impedance
- extended-reacting ground
  $\Longrightarrow$ propagation of the acoustic waves into the ground is computed

Impedance boundary condition

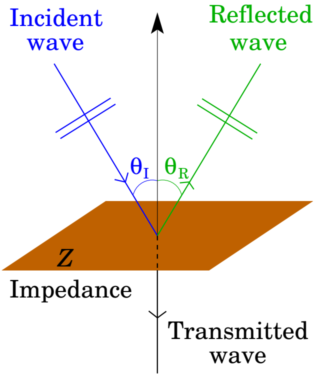

Propagation into the ground

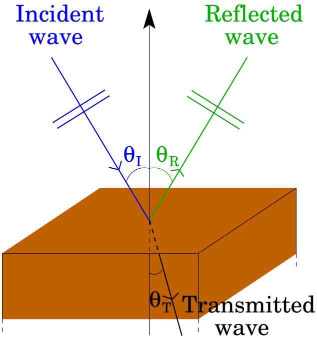

Impedance boundary condition (1)

Surface impedance

- caracterize the reflexion of waves over a surface: absorption and phase shift
- for natural grounds, use mainly of semi-empirical models, with a single parameter

frequency domain | time domain

$$P(\omega) = Z(\omega)V(\omega) \qquad \Longrightarrow \qquad p(t) = \int_{-\infty}^{+\infty} z(t-t')v(t')\mathrm{d}t'$$

Impedance models proposed in the literature developed in the frequency domain

$\Longrightarrow$ translation in the time domain?

Not straightforward:

- some physical conditions, such as causality, “lost” in the frequency domain
- widely used models, such as the one proposed by Delany and Bazley are deduced from measurements

Some references from the literature in acoustics:

- Miki [14]: modification of the Delany and Bazley model
- Rienstra [15]: three necessary conditions to formulate the impedance boundary condition in the time-domain

Impedance boundary condition (2)

Three necessary conditions in Rienstra [15]:

1. **reality** condition $Z^*(\omega) = Z(-\omega)$ in the complex plane
2. **passivity** condition $\mathrm{Re}[Z(\omega)] \geq 0$ for $\omega > 0$
3. **causality** condition $z(t) = 0$ for $t < 0$

Remarks:

- condition similar to those defining a positive-real function in circuit analysis
- impedance is not a transfer function:
  $\Longrightarrow$ the causality condition should also be check for the admittance (Rienstra)
- real quantity of interest: reflexion coefficient?

Recent study to investigate these conditions for the impedance models used in outdoor sound propagation in Dragna & Blanc-Benon [16]:

- semi-infinite ground $Z = Z_c$

- rigidly-backed layer $Z = Z_c \coth(-\mathrm{i}k_c d)$

Some results:

- physically-based models (Zwikker and Kosten, Hamet and Bérengier, variable porosity) are physically admissible
- Delany and Bazley (in its usual form) is not causal
- Miki model for a rigidly-backed layer is not passive at low frequencies
- proposition of a modified Miki model that is passive

Surface impedance for a rigidly-backed layer:

— Delany and Bazley

- - - Miki

- · - modified Miki

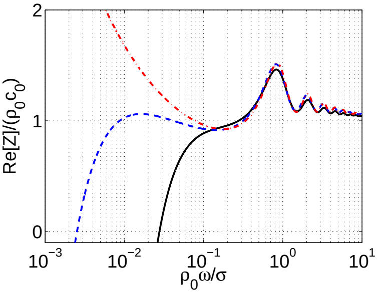

Other study done by Kirby in [17]

- retrieves that the Miki model is not passive
- shows also that the real part of the density is negative at low frequencies

Additional study in Dragna, Attenborough & Blanc-Benon [18]

- the real part of the density is also negative at low frequencies for the modified Miki model

Real part of the density for a porous medium:

— Delany and Bazley

- - - Miki

- · - modified Miki

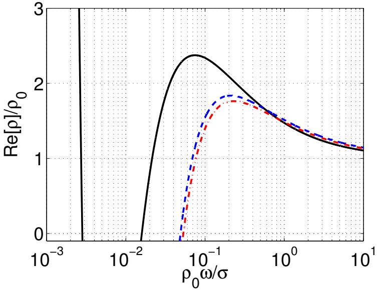

Summary:

- semi-empirical models can be modified to be admissible for a particular case
- in the general case, the surface impedance would however not be physical
- physical-based models yield comparable results and must be preferred

Naive approche to evaluate $p(t) = [v * z](t) = \int_{-\infty}^{t} v(t')z(t-t')\,\mathrm{d}t'$

$\Longrightarrow$ requires a large memory space and CPU time for long-range propagation

Lot of works in the literature to develop efficient convolution methods (e.g. [19-23])

Time-domain impedance boundary condition (TDIBC) suitable for high-order solver in Troian et al. [24]

1. **Approximate $Z(\omega)$ by a rational function**

$$Z(\omega) \approx Z_P(\omega) = Z_\infty + \frac{a_0 + a_1(-\mathrm{i}\omega) + \ldots + a_{P-1}(-\mathrm{i}\omega)^{P-1}}{1 + b_1(-\mathrm{i}\omega) + \ldots + b_P(-\mathrm{i}\omega)^P}$$

Decomposition into partial fractions

$$Z_P(\omega) = Z_\infty + \sum_{k=1}^{N} \frac{A_k}{\lambda_k - \mathrm{i}\omega} + \sum_{k=1}^{M} \frac{1}{2}\left[\frac{B_k + \mathrm{i}C_k}{\alpha_k + \mathrm{i}\beta_k - \mathrm{i}\omega} + \frac{B_k - \mathrm{i}C_k}{\alpha_k - \mathrm{i}\beta_k - \mathrm{i}\omega}\right]$$

with corresponding time response:

$$z(t) \approx Z_\infty\delta(t) + \sum_{k=1}^{N} A_k \mathrm{e}^{-\lambda_k t}\mathrm{H}(t) + \sum_{k=1}^{M} \mathrm{e}^{-\alpha_k t}[B_k\cos(\beta_k t) + C_k\sin(\beta_k t)]\mathrm{H}(t)$$

instantaneous response   first-order system response   second-order system response

2. Formulation of the convolution by a set of first-order differential equations

For that, introducing $z(t)$ into the convolution leads to:

$$p(t) = Z_\infty v(t) + \sum_{k=1}^{N} A_k \phi_k(t) + \sum_{k=1}^{M} [B_k \psi_k^{(1)}(t) + C_k \psi_k^{(2)}(t)] \qquad (1)$$

where the new variables, called accumulators, bring the information of the convolution:

$$\phi_k(t) = \int_{-\infty}^{t} v(t') \mathrm{e}^{-\lambda_k (t-t')} \mathrm{d}t'$$

$$\psi_k^{(1)}(t) = \int_{-\infty}^{t} v(t') \mathrm{e}^{-\alpha_k (t-t')} \cos(\beta_k (t-t')) \mathrm{d}t'$$

$$\psi_k^{(2)}(t) = \int_{-\infty}^{t} v(t') \mathrm{e}^{-\alpha_k (t-t')} \sin(\beta_k (t-t')) \mathrm{d}t'$$

Time-variations of the accumulators governed by first-order differential equations:

$$\frac{\mathrm{d}\phi_k}{\mathrm{d}t} + \lambda_k \phi_k(t) = v(t) \qquad (2)$$

$$\frac{\mathrm{d}\psi_k^{(1)}}{\mathrm{d}t} + \alpha_k \psi_k^{(1)}(t) - \beta_k \psi_k^{(2)}(t) = p(t) \qquad (3) \qquad\qquad \frac{\mathrm{d}\psi_k^{(2)}}{\mathrm{d}t} + \alpha_k \psi_k^{(2)}(t) + \beta_k \psi_k^{(1)}(t) \qquad (4)$$

$\Longrightarrow$ TDIBC imposed with (1) with accumulators obtained by solving (2)-(4)

Example of rational approximations of the surface impedance:

- Hamet and Bérengier impedance model [25]
- rational approximation with $N = 2$ and $M = 0$ over the frequency band 50-800 Hz

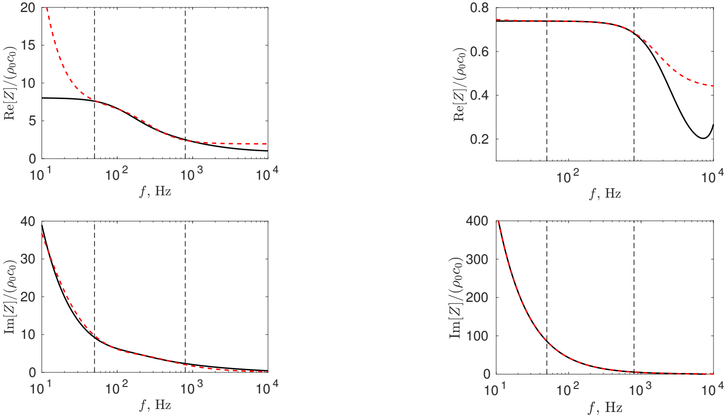

semi-infinite ground of flow resistivity 100 kPa s m^{-2}

rigidly backed layer of flow resistivity 10 kPa s m^{-2} and thickness 1 cm

Propagation into the ground

Ground usually assumed to be a porous medium with a rigid frame

$\Longrightarrow$ can be treated as an equivalent fluid with frequency-dependent properties

frequency domain

$$-\mathrm{i}\omega P + K_g(\omega)\nabla\cdot\mathbf{V} = 0$$

$$-\mathrm{i}\omega\rho_g(\omega)\mathbf{V} + \nabla P = 0$$

$\Longrightarrow$

time domain

$$\frac{\partial p}{\partial t} + [K_g * \nabla\cdot\mathbf{v}](t) = 0$$

$$\left[\rho_g * \frac{\partial \mathbf{v}}{\partial t}\right](t) + \nabla p = 0$$

$K_g = \omega Z_c/k_c$ compressibility and $\rho_g = Z_c k_c/\omega$ density

Examples of equations obtained for two models;

- equations based on the Zwikker and Kosten model [2, 27]

$$\frac{\partial \mathbf{v}}{\partial t} + \frac{\Omega}{\rho_0 q^2}\nabla p + \frac{\sigma_0\Omega}{\rho_0 q^2}\mathbf{v} = 0 \qquad \frac{\partial p}{\partial t} + \frac{\rho_0 c^2}{\Omega}\nabla\cdot\mathbf{v} = 0$$

  equations without convolutions but limited applications [28]

- equations based on the Wilson's relaxation model [28]

$$\frac{\partial \mathbf{v}}{\partial t} + \frac{\Omega}{\rho_0 q^2}\left[s^v * \nabla p\right] + \frac{1}{\tau_v}\mathbf{v} = 0 \qquad \frac{\partial p}{\partial t} + \frac{\rho_0 c^2}{\Omega}\left[s^e * \nabla\cdot\mathbf{v}\right] = 0$$

- equations based on the Johnson-Champoux-Allard model [29]

Convolutions can be computed using the same method than impedance [30]

Application on a 3D case (1)

Propagation of an acoustic impulse into an inhomogeneous atmosphere

- sound speed profile $c(z) = c_0 + A_c \ln \frac{z + z_0}{z_0}$ with $A_c = 2$ m s^{-1} and $z_0 = 0.1$ m

Ground: a rigidly backed layer of thickness 0.1 m with two set of parameters:

- a soft ground with $\sigma_0 = \mathbf{10}$ kPa s m^{-2}, $q = 1.8$, $\Omega = 0.5$ and $s_B = 1$
- a harder ground with $\sigma_0 = \mathbf{200}$ kPa s m^{-2}, $q = 1.8$, $\Omega = 0.5$ and $s_B = 1$

Three different ground modelling:

- Zwikker and Kosten propagation equations (equations without convolutions)
- Wilson's equations (equations with convolutions)
- an impedance boundary condition using the Wilson's relaxation model

Numerical specification

- domain: [-5 m; 155 m]$\times$ [-6.6 m; 6.6 m] $\times$ [-0.1 m; 25 m]
- moving frame
- $\approx$ 140 million of points

Ground with $\sigma_0 = \mathbf{10}$ kPa s m^{-2}

Observer at $x = 150$ m, $y = 0$ m and $z = 2$ m

- Fair agreement between the results for the impedance boundary condition and for Wilson's equations
  $\Longrightarrow$ extended reaction required
- Results obtained with the Zwikker and Kosten and Wilson's equations dramatically different

Zwikker and Kosten equations

Wilson's equations

Wilson's impedance model

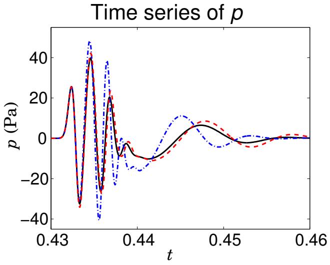

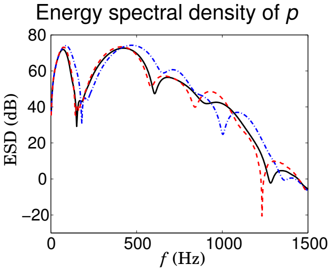

Ground with $\sigma_0 = \mathbf{200}$ kPa s m^{-2}

Observer at $x = 150$ m, $y = 0$ m and $z = 2$ m

- Results obtained with the impedance boundary condition match closely those with Wilson's equations
  $\Longrightarrow \sigma_0$ high enough so that local reaction can be assumed
- Small discrepancies remain between the results obtained with the Zwikker and Kosten and with the Wilson's equations

Zwikker and Kosten equations

Wilson's equations

Wilson's impedance model

Time series of p

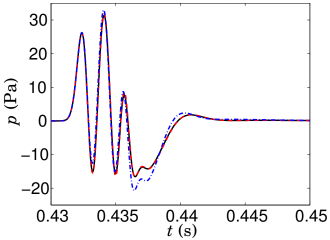

Energy spectral density of p

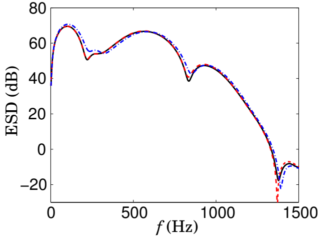

Reflexion over an absorbing ground: Summary

Time-domain impedance boundary condition

- use of a rational to approximate the impedance
  - few poles usually required
  - accurate approximation
- computation of the convolution replaced by integration of first-order differential equation
- well-suited for high-order methods

Time-domain propagation equations in the ground

- convolutions that can be evaluated as the impedance BC
- required if the ground is extended-reacting
- equations obtained up to now for some impedance models

A structured grid is necessary for finite difference methods
$\Longrightarrow$ accounting for a non flat ground is not straightforward

Non-flat terrain profile $H(x, y)$

Change of variable: [30]

$z \rightarrow z + H(x, y)$

$$\frac{\partial}{\partial x} \rightarrow \frac{\partial}{\partial x} - \frac{\partial H}{\partial x}\frac{\partial}{\partial z}$$
$$\frac{\partial}{\partial y} \rightarrow \frac{\partial}{\partial y} - \frac{\partial H}{\partial y}\frac{\partial}{\partial z}$$
$$\frac{\partial}{\partial z} \rightarrow \frac{\partial}{\partial z}$$

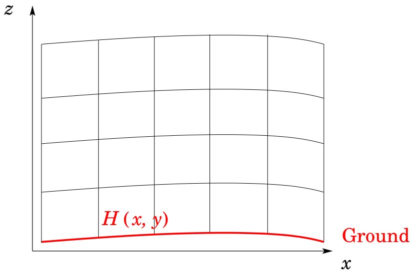

Generalization: **curvilinear coordinates** [31]

Physical domain (x, y, z) $\Longleftrightarrow$ Computational domain (ξ, ζ, η)

Method used in computational aeroacoustics [32]

Topography: curvilinear coordinates (2)

Physical domain

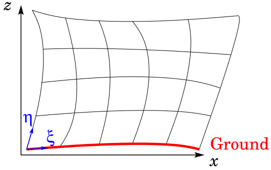

Computational domain

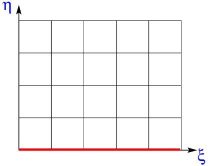

Linearized Euler equations:

Cartesian case — curvilinear case

$$\frac{\partial \mathbf{U}}{\partial t}+\frac{\partial \mathbf{E}}{\partial x}+\frac{\partial \mathbf{F}}{\partial y}+\frac{\partial \mathbf{G}}{\partial z}+\mathbf{H}=\mathbf{S} \quad \Longrightarrow \quad \frac{\partial \mathbf{U}^*}{\partial t}+\frac{\partial \mathbf{E}^*}{\partial \xi}+\frac{\partial \mathbf{F}^*}{\partial \zeta}+\frac{\partial \mathbf{G}^*}{\partial \eta}+\mathbf{H}^*=\mathbf{S}^*$$

$$\mathbf{E}^*=\frac{\xi_x\mathbf{E}+\xi_y\mathbf{F}+\xi_z\mathbf{G}}{J},\quad \mathbf{F}^*=\frac{\zeta_x\mathbf{E}+\zeta_y\mathbf{F}+\zeta_z\mathbf{G}}{J},\quad \mathbf{G}^*=\frac{\eta_x\mathbf{E}+\eta_y\mathbf{F}+\eta_z\mathbf{G}}{J},$$

$$\mathbf{U}^*=\frac{\mathbf{U}}{J},\quad \mathbf{H}^*=\frac{\mathbf{H}}{J}\ \text{ et }\ \mathbf{S}^*=\frac{\mathbf{S}}{J}.$$

J: jacobian of the geometrical transformation

ξ_x, ξ_y, ...: metrics of the transformation ($\xi_x = \partial xi/\partial x$)

Topography: curvilinear coordinates (3)

Summary:

- same numerical methods than for a flat ground
- nonflat terrains even with large slopes (around 45°) can be accounted for
- the geometrical transformation, and a fortiori the terrain profile has to be smooth (no slope discontinuities)

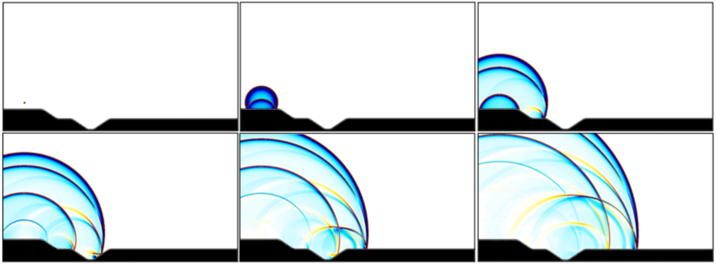

Other approaches are required for a more general description of the boundary

- immersed boundary method for structured grid?
- unstructured grids well-suited

With the LEEs, mean field of T_0 and V_0 can be taken into account and their effect on the acoustic field investigated:

- using analytical profiles
  - vertical linear or logarithmic profiles [33, 34]
  - profiles from the Monin-Obukhov similarity theory
- using profiles obtained from numerical simulation
  - solvers of the fluid mechanics equations [1,26]
  - meteorological models (see Aumond *et al.* [35])

Example: effect of the wind on the efficiency of noise barriers in Van Renterghem & Botteldooren [26]

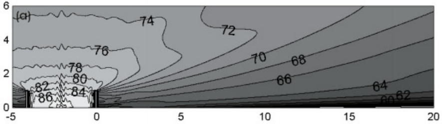

without wind

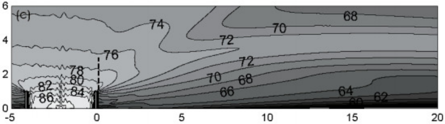

with wind

Turbulent field

Fluctuations :

- temperature T (through c_0) : scalar field
- velocity $\mathbf{V}$: vector field

Synthetic turbulence

- generated via Fourier modes or related methods [36-38]

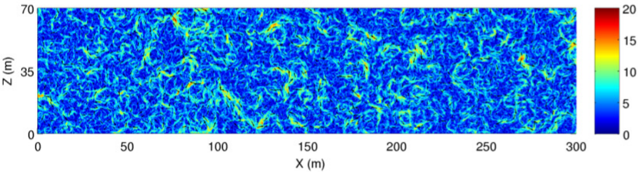

Fluctuations of wind velocites generated by the random fluctuations generation (RFG) algorithm in Ehrhardt *et al.* [38]

Example: diffusion by a volume of turbulence

Temperature fluctuations at the center of the domain with a von Kármán spectra [37]

Harmonic plane wave with $f = 100$ Hz

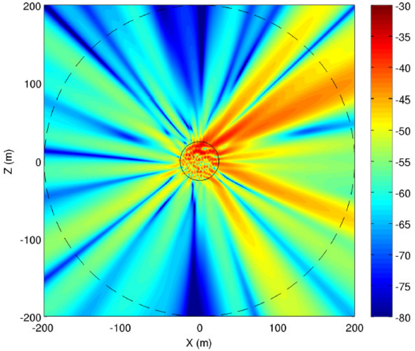

Sound pressure level relative(dB) to the incident field $20\log_{10}(|p_1|/|p_0|)$

Scattering cross-section

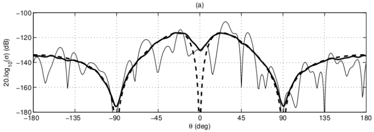

numerical solution:

— single realization

— ensemble-averaging over 200 realizations

- - - theory in far-field

Description of the experimental site

Measurements on the railway site near La Veuve in May 2010:

- Topography
- Surface impedances
- Meteorological conditions

Campaign carried out with:

- SNCF test department
- Institut Français des Sciences et Technologies des Transports, de l'Aménagement et des Réseaux (IFSTTAR)

Impulsive source: blank pistol shots

Receivers located at: 7.5 m, 25 m and 100 m

Comparison with numerical simulation in [39]

Propagation line

Gap in near-field

Site modelling: topography

Topography measurement done by the SNCF test department

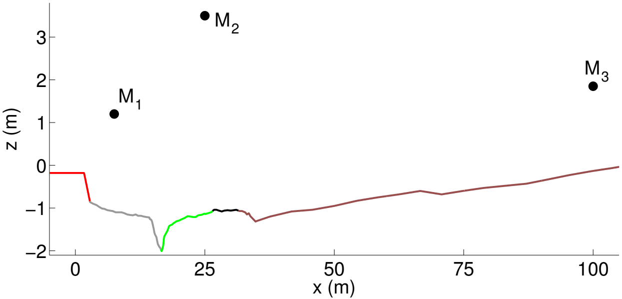

Ground profile relatively flat

Gap at $x = 18$ m whose depth is 0.8 m

Five types of ground impedances

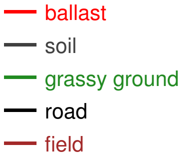

Site modelling: surface impedances

In situ measurement using the **transfer function method**

Road: perfectly reflecting ground

Soil, grassy ground and field:
Miki model of a rigidly backed layer [14]

Ballast:

- measurement difficult on the experimental due to reflexions on rails
- additional measurement realized on the IFSTTAR's site in Bouguenais
- Hamet and Bérengier impedance model [25]

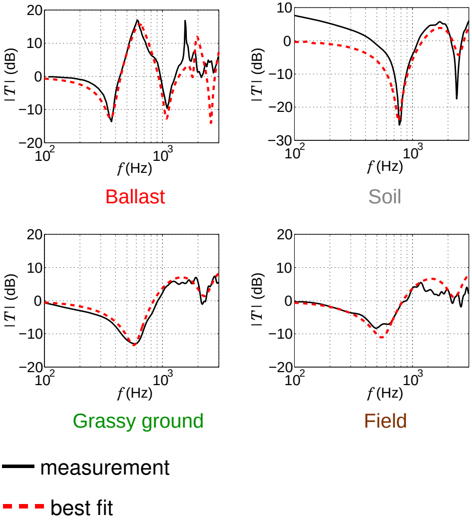

Impulsive source: blank pistol shots

Source located at $z_S = 1$ **m**

3 shots

Positioning error

Results for the three shots

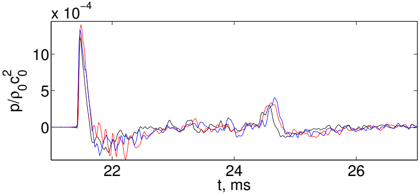

Waveforms

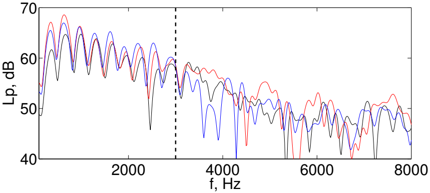

Sound pressure levels

$\Longrightarrow$ **Comparisons up to 3000 Hz**

Meteorological mast located at 125 m from the center of the railway track:

- propeller anemometers and temperature sensors at heights of 1 m, 3 m and 10 m
- sonic anemometer at a height of 10 m
- humidity sensor at a height of 3 m

Downwind conditions

Profiles determined with the Monin-Obukhov similitude theory

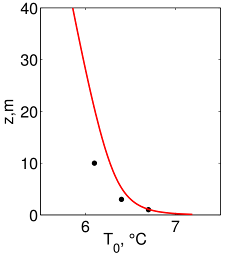

Temperature

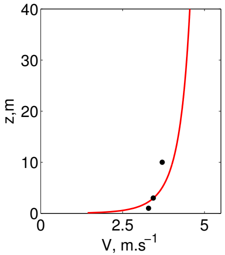

Wind speed

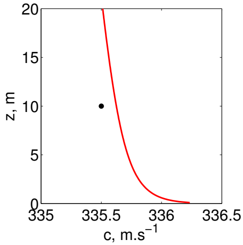

Sound speed

• measurements — Monin-Obukhov profile

Numerical specification

2-D Simulations

- linearized Euler equations in curvilinear coordinates
- optimized finite difference schemes of Bogey & Bailly [9]
- mesh sizes $\Delta\xi = \Delta\eta = 0.01$ m with 11000 and 1500 points respectively in the ξ-direction and in the η-direction
- CFL $= 0.6$ and 22000 time iterations

Curvilinear transformation:

$$x = \xi,$$
$$z = \eta + H(\xi),$$

with ground profile $H(\xi)$ approximated by splines

Correction 2D/3D [40]

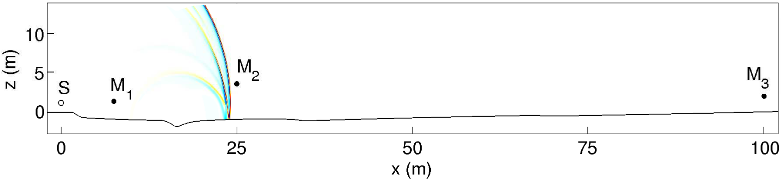

Snapshot of the acoustic pressure at $t = 71$ ms

Comparison of the results: time domain

— measurement

- - - numerical prediction

- · - numerical prediction with time-alignment

At the receiver M_1:

- arrival time of the direct wave well predicted
- arrival time and amplitude of the reflected wave well predicted

At the receiver M_2:

- small time delay between the measurement and the numerical prediction
- good agreement between the waveforms

At the receiver M_3:

- larger time delay
- shape of the waveforms are similar

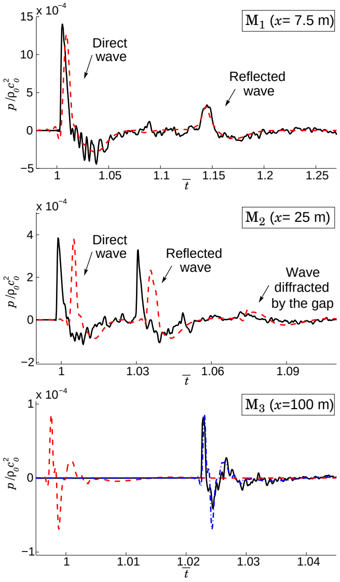

Waveforms

Comparison of the results: frequency domain

— measurement

- - - numerical prediction

Good overall agreement up to 2 kHz

Position of interference patterns well-predicted

Sound exposure level (SEL):

$$\text{SEL} = 10\log_{10} \int_{-\infty}^{+\infty} \frac{p(t)^2}{p_{\text{ref}}^2}\,\mathrm{d}t$$

with $p_{\text{ref}} = 210^{-5}$ Pa

SEL	experimental result	numerical prediction
M_1 $x = 7.5$ m	101.1 dB	100.5 dB
M_2 $x = 25$ m	92.2 dB	92.0 dB
M_3 $x = 100$ m	79.3 dB	79.1 dB

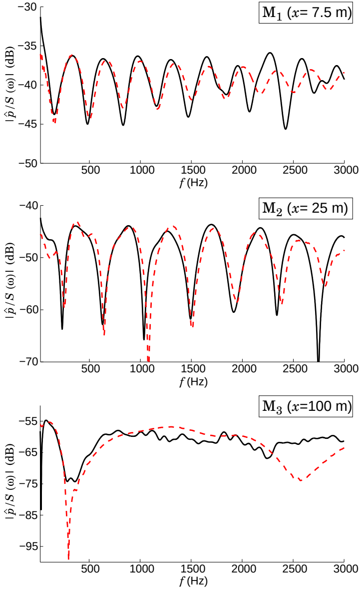

Normalized energy spectral densities

Moving source above an absorbing ground

Analytical solutions known only in simple cases

- source moving at a constant height and constant speed above a flat ground in a homogeneous atmosphere [41-44]

Time-domain approaches well-suited for studying the radiation of moving sources: [45]

- broadband source, with any trajectory possible
- broadband formulation for the surface impedance

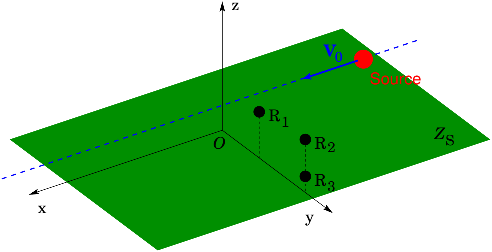

Source speed $V_0 = 50$ m.s^{-1} and height $z = 2$ m

Source $S(\mathbf{x}, t) = Q(\mathbf{x} - \mathbf{V_0}t)s(t)$

3D simulation

Results: perfectly reflecting ground

Spectrogram of the acoustic pressure at the observer
located at R_1 - $x = 0$ m, $y = 5$ m, $z = 3$ m, dB/Hz

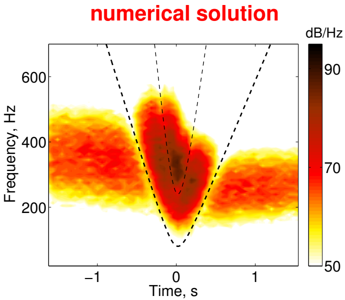

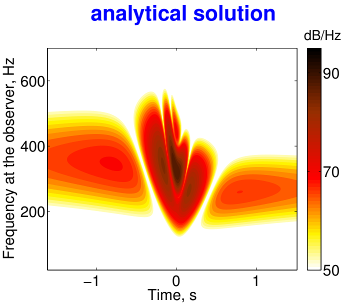

Doppler effect

Interference when $R_{e,2} - R_{e,1} = (1/2 + n)\lambda$, n integer

- $R_{e,1}$ distance between the source and the observer at the emission time
- $R_{e,2}$ distance between the image source and the observer at the emission time

Analytical solution: source + image source

Excellent agreement between the analytical and numerical solutions

Spectrogram of the acoustic pressure at the observer located at R_1 - $x = 0$ m, $y = 5$ m, $z = 3$ m, dB/Hz

perfectly relfecting ground

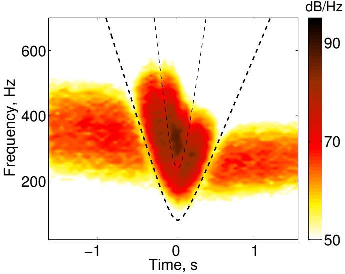

absorbing ground

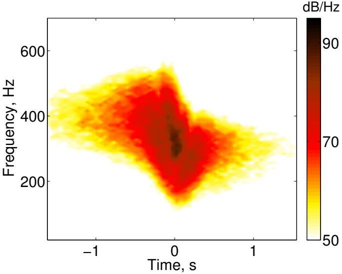

Destructive interferences suppressed

PSD lower for the absorbing ground when the source is far from the observer

$$\text{Sound pressure level } \mathrm{SPL}(\mathbf{x}, t) = \int_0^{+\infty} \mathrm{DSP}(\mathbf{x}, f, t)\mathrm{d}f, \text{ dB}$$

$\mathbf{R}_1$ - $x = 0$ m, $y = 5$ m, $z = 3$ m

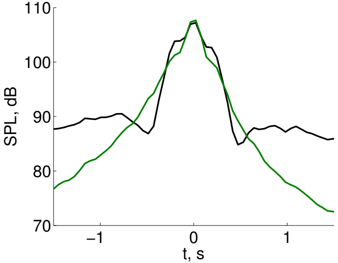

$\mathbf{R}_3$ - $x = 0$ m, $y = 25$ m, $z = 0.5$ m

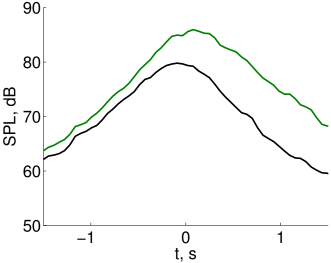

— perfectly reflecting ground — absorbing ground

Perfectly reflecting ground:

- SPL higher when the source approaches the receiver ($t < 0$): convective amplification

Absorbing ground:

- not always the case
  $\Longrightarrow$ competition between ground absorption and convective amplification

Conclusions

Time-domain approaches well-suited for atmospheric sound propagation

- broadband computation
- pulse signals
- sources in motion

Solving linearized Euler equations:

- possible to account for most of the important physical phenomena
- possible to use hybrid approaches with more efficient methods for long range

The same numerical methods can be used for nonlinear propagation in the atmosphere [4]

Perspectives:

- better description of the source
  - radiation of vibrating bodies at rest or in motion
  - aerodynamic source: coupling with a large-eddy simulations code, that gives the acoustic field generated by the source region
- better description of the atmosphere
  - including time-varying wind and temperature fields obtained by large-eddy simulations
- including atmospheric absorption (especially relaxation effects)

References: numerical methods (1)

General references:

[1] Blumrich R. & Heimann D., (**2002**), “A linearized Eulerian (LE) sound propagation model for studies of complex meteorological effects”, *J. Acoust. Soc. Am.* **112**, 446-455.

[2] Salomons, E., Blumrich R. & Heimann D., (**2002**), “Eulerian Time-Domain Model for Sound Propagation over a Finite-Impedance Ground Surface. Comparison with Frequency-Domain Models ”, *Acta Acust. united Ac.* **88**, 483-492. *J. Acoust. Soc. Am.* **112**, 446-455.

[3] Ostashev V.E., Wilson D.K., Liu L., Aldridge D.F., Symons, N.P. & Marlin, D., (**2005**), “Equations for finite-difference, time-domain simulation of sound propagation in moving inhomogeneous media and numerical implementation”, *J. Acoust. Soc. Am.* **117**, 503-517.

Examples of numerical studies:

[4] Sabatini R., Marsden O., Bailly C. & Bogey C., (**2016**), “A numerical study of nonlinear infrasound propagation in a windy atmosphere”, *J. Acoust. Soc. Am.*, **140**, 641-656.

[5] Yamashita R. & Suzuki K., (**2016**), “Full-Field Sonic Boom Simulation in Stratified Atmosphere”, *AIAA J.* **54**, 3223-3231.

[6] Guillaume G., Aumond P., Gauvreau B. & Dutilleux G., (**2014**). “Application of the transmission line matrix method for outdoor sound propagation modelling – Part 1: Model presentation and evaluation”, *Appl. Acoust.* **76**(2), 113–118.

[7] Hornikx M., Waxler R. & Forssén J., (**2010**), “The extended Fourier pseudospectral time-domain method for atmospheric sound propagation”, *J. Acoust. Soc. Am.* **128**(4), 1632–1646.

References: numerical methods (2)

Finite difference schemes and time-integration:

[8] Tam C.K.W. & Webb J.C., (**1993**), "Dispersion-relation preserving finite difference schemes for computational acoustics", *J. Comp. Phys.* **107**, 262–281.

[9] Bogey C. & Bailly C., (**2004**), "A family of low dispersive and low dissipative explicit schemes for noise computation", *J. Comp. Phys.* **194**, 194-214.

Non-reflecting boundary conditions:

[10] Bérenger J.P., (**1994**), "A perfectly matched layer for the absorption of electromagnetic waves", *J. Comp. Phys.* **114**, 185–200.

[11] Tam C.K.W. & Dong Z., (**1996**), "Radiation and outflow boundary conditions for direct computation of acoustic and flow disturbances in a nonuniform mean flow.", *J. Comput. Acoust.* **4**, 175–201.

[12] Bogey C. & Bailly C., (**2002**), "Three-dimensional non-reflective boundary conditions for acoustic simulations: far field formulation and validation test cases", *Acta Acust. united Ac.* **88**(4), 463–471.

LEE-PE coupling:

[13] Van Renterghem T., Salomons E. & Botteldooren D., (**2005**), "Efficient FDTD-PE model for sound propagation in situations with complex obstacles and wind profiles", *Acta Acust. united Ac.* **91**, 671–679.

References: interaction with the ground (1)

Admissibility conditions for an impedance model:

[14] Miki Y., (**1990**), “Acoustical properties of porous materials - Modifications of Delany-Bazley models”, *J. Acoust. Soc. Jpn.* **11**(1), 19–24.

[15] Rienstra S., (**2006**), “Impedance models in time domain, including the extended Helmholtz resonator model”, *12th AIAA/CEAS Aeroacoustics Conference*, Cambridge, MA, USA, 8-10 May 2006, AIAA 2006-2686,.

[16] Dragna D. & Blanc-Benon P., (**2014**), “Physically admissible impedance models for time-domain computations of outdoor sound propagation”, *Acta Acust. united Ac.* **100**, 401-410.

[17] Kirby R., (**2014**), “On the modification of Delany and Bazley fomulae”, *Appl. Acoust.* **86**, 47-49.

[18] Dragna D., Attenborough K. & Blanc-Benon P., (**2015**), “On the inadvisability of using single parameter impedance models for representing the acoustical properties of ground surfaces”, *J. Acoust. Soc. Am.* **138**, 2399-2413.

Time-domain impedance boundary condition:

[19] Botteldooren D., (**1995**). “Finite-difference time-domain simulation of low-frequency room acoustic problems”, *J. Acoust. Soc. Am.* **98**(6), 3302–3308.

[20] Heutschi K., Horvath M. & Hofmann J., (**2005**). “Simulation of ground impedance in finite difference time domain calculations of outdoor sound propagation”, *Acta Acustica united with Acustica*, **91**, 35–40.

[21] Ostashev V.E., Collier S.L., Wilson D.K., Aldridge D.F., Symons N.P. & Marlin D.H. (**2007**), “Padé approximation in time-domain boundary conditions of porous surfaces”, *J. Acoust. Soc. Am.* **122**(1), 107–112.

References: interaction with the ground (2)

[22] Reymen Y., Baelmans M. & Desmet W., (**2006**). “Time-Domain Impedance Formulation based on Recursive Convolution”, *12th AIAA/CEAS Aeroacoustics Conference*, Cambridge, MA, USA, 8-10 May 2006, AIAA Paper 2006-2685.

[23] Cotté B., Blanc-Benon P., Bogey C. & Poisson, F., (**2009**). “Time-domain impedance boundary conditions for simulations of outdoor sound propagation”, *AIAA J.* **47**, 2391–2403.

[24] Troian R., Dragna D., Bailly C. & Galland M.A., (**2017**), “Broadband liner impedance eduction for multimodal acoustic propagation in the presence of a mean flow”, *J. Sound Vib.* **392**, 200-216.

Surface impedance model:

[25] Bérengier M., Stinson M.R., Daigle G.A. & Hamet J.F., (**1997**). "Porous road pavement: Acoustical characterization and propagation effects“, *J. Acoust. Soc. Am.* **101**, 155–162.

Propagation equations in the ground:

[26] Van Renterghem T. & Botteldooren D. (**2003**), “Numerical simulation of the effect of trees on downwind noise barrier performance”, *Acta Acustica united with Acustica* **89**, 764–778.

[27] Wilson D.K., Ostashev V. E., Collier S.L., Symons N.P., Aldridge D.F. & Marlin, D.H., (**2007**), “Time-domain calculations of sound interactions with outdoor ground surfaces”, *Appl. Acoust.* **68**(2), 173–200.

[28] Umnova O. & Turo D., (**2009**), “Time domain formulation of the equivalent fluid model for rigid porous media”, *J. Acoust. Soc. Am.* **125**, 1860–1863.

[29] Dragna D., Pineau P. & Blanc-Benon P., (**2015**), “A generalized recursive convolution method for time-domain propagation in porous media”, *J. Acoust. Soc. Am.* **138**, 1030-1042.

References: interaction topography/inhomogeneous atmosphere

Topography:

[30] Heimann D. & Karle R., (**2006**). "A linearized Euler finite-difference time-domain sound propagation model with terrain-following coordinates", *J. Acoust. Soc. Am.* **119**(6), 3813–3821.

[31] Dragna D., Blanc-Benon P. & Poisson F., (**2013**). "Time-domain solver in curvilinear coordinates for outdoor sound propagation over complex terrain", *J. Acoust. Soc. Am.* **133**(6), 3751-3763.

[32] Marsden O., Bogey C. & Bailly C., (**2005**), "High-order curvilinear simulations of flows around non-Cartesian bodies", *J. Comp. Acous.* **13**, 731-748.

Mean field:

[33] Cotté B. & Blanc-Benon, P., (**2009**), "Time-domain simulations of sound propagation in a stratified atmosphere over an impedance ground", *J. Acoust. Soc. Am.* (**125**(5), EL 202-207.

[34] Dragna D., Cotté B., Blanc-Benon P. & Poisson F., (**2011**). "Time-domain simulations of outdoor sound propagation with suitable impedance boundary conditions", *AIAA J.* **49**, 1420–1428.

[35] Aumond P., Guillaume G., Gauvreau B., Lac C., Masson V. & Bérengier M., (**2014**) "Application of the Transmission Line Matrix method for outdoor sound propagation modelling – Part 2: Experimental validation using meteorological data derived from the meso-scale model Meso-NH", *Appl. Acoust.* **76**(2), 107–112.

Turbulent field:

[36] Frehlich R., Cornman L. & Sharman R., (**2001**), "Simulation of three-dimensional turbulent velocity fields", *J. Appl. Meteorol.* **40**, 246–258.

[37] Cheinet S., Ehrhardt L., Juvé D. & Blanc-Benon P., (**2012**), "Unified modeling of turbulence effects on sound propagation", *J. Acoust. Soc. Am.* **132**(4), 2198-2209.

[38] Ehrhardt L., Cheinet S., Juvé D. & Blanc-Benon P., (**2013**), "Evaluating a linearized Euler equations model for strong turbulence effects on sound propagation", *J. Acoust. Soc. Am.* **133**(4), 1922-1933.

Comparison with experimental data:

[39] Dragna D., Blanc-Benon P. & Poisson F., (**2010**), "Impulse propagation over a complex site: A comparison of experimental results and numerical predictions", *J. Acoust. Soc. Am.* **135**(3), 1096-1105.

[40] Parakkal S., Gilbert K.E., Di, X. & Bass H.E., (**2010**), "A generalized polar coordinate method for sound propagation over large-scale irregular terrain", *J. Acoust. Soc. Am.* **128**(5), 2573–2580.

Moving source:

[41] Norum T.D. & Liu C.H., (**1978**), "Point source moving above a finite impedance reflecting plane-experiment and theory", *J. Acoust. Soc. Am.* **63**(4), 1069-1073.

[42] Oie S. & Takeuchi R., (**1981**), "Sound radiation from a point source moving in parallel to a plane surface of porous material", *Acustica* **48**(3), 123-129.

[43] Ochmann M., (**2013**). "Exact solutions for sound radiation from a moving monopole above an impedance plane", *J. Acoust. Soc. Am.*, **133**(4), 1911–1921.

[44] Attenborough K., Li K.M. & Horoshenkov K., (**2007**), *Predicting Outdoor Sound*, Taylor & Francis, London and New York.

[45] Dragna D. & Blanc-Benon P., (**2015**), "Sound radiation by a moving line source above an impedance plane with frequency-dependent properties", *J. Sound Vib.* **349**, 259-275.

[46] Dragna D., Blanc-Benon P. & Poisson F., (**2014**), "Modeling of broadband moving sources for time-domain simulations of outdoor sound propagation", *AIAA J.* **52**, 1928-1939.